

## A passive-flow microfluidic device for imaging latent HIV activation dynamics in single T cells

Ramesh Ramji, Victor C. Wong, Arvind K. Chavali, Larisa M. Gearhart, and Kathryn Miller-Jensen\*

### Electronic Supplementary Information

**Figure S1.** Scanning electron microscope (SEM) images of S and V traps.

**Figure S2.** Effect of cell loading density and volume on cell trapping efficiency.

**Figure S3.** Drug-stimulated latent HIV activation in the passive-flow device is similar to behavior observed in plate-based flow cytometry assays.

**Figure S4.** Trends in the CV for  $t_{on}$  are consistent at longer stimulation times.

**Figure S5.** CVs for  $t_{on}$ ,  $F_{maxO}$ , and slope are consistent between cell cycle synchronized and unsynchronized cells after PMA treatment.

**Figure S6.** Three metrics that describe HIV expression are strongly correlated.

**Figure S7.** Trends between different treatments are similar with and without the quantification of non-activators.

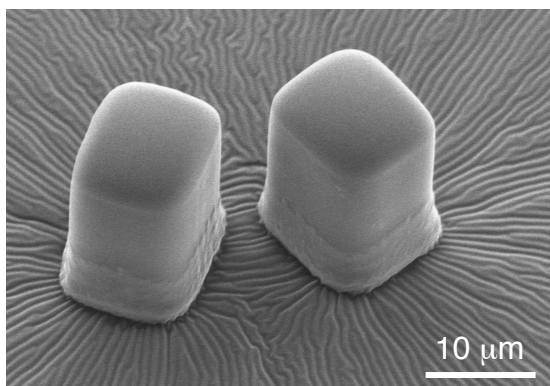
**Table S1.** Analysis of distributions for onset of activation time ( $t_{on}$ ), maximum HIV expression ( $F_{maxO}$ ), and rate of HIV production (slope) demonstrates statistically significant differences in reactivation dynamics.

**Movie S1.** Comparison of docking of Jurkat cells treated with PMA in the microfluidic device versus poly-lysine-coated plate. Time stamp in hours:minutes (00:00).

**Movie S2.** Solution delivery within the microfluidic device. Time stamp in seconds.

**Movie S3.** Cell loading in the microfluidic device. Time stamp in minutes:seconds (00:00).

S trap



V trap

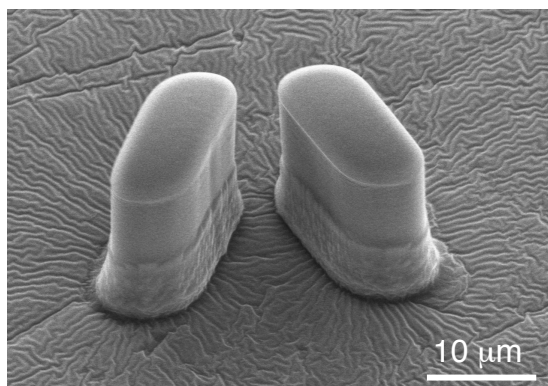


**Fig. S1.** Scanning electron microscope (SEM) images of square pillars (S traps) and rectangular pillars (V traps).

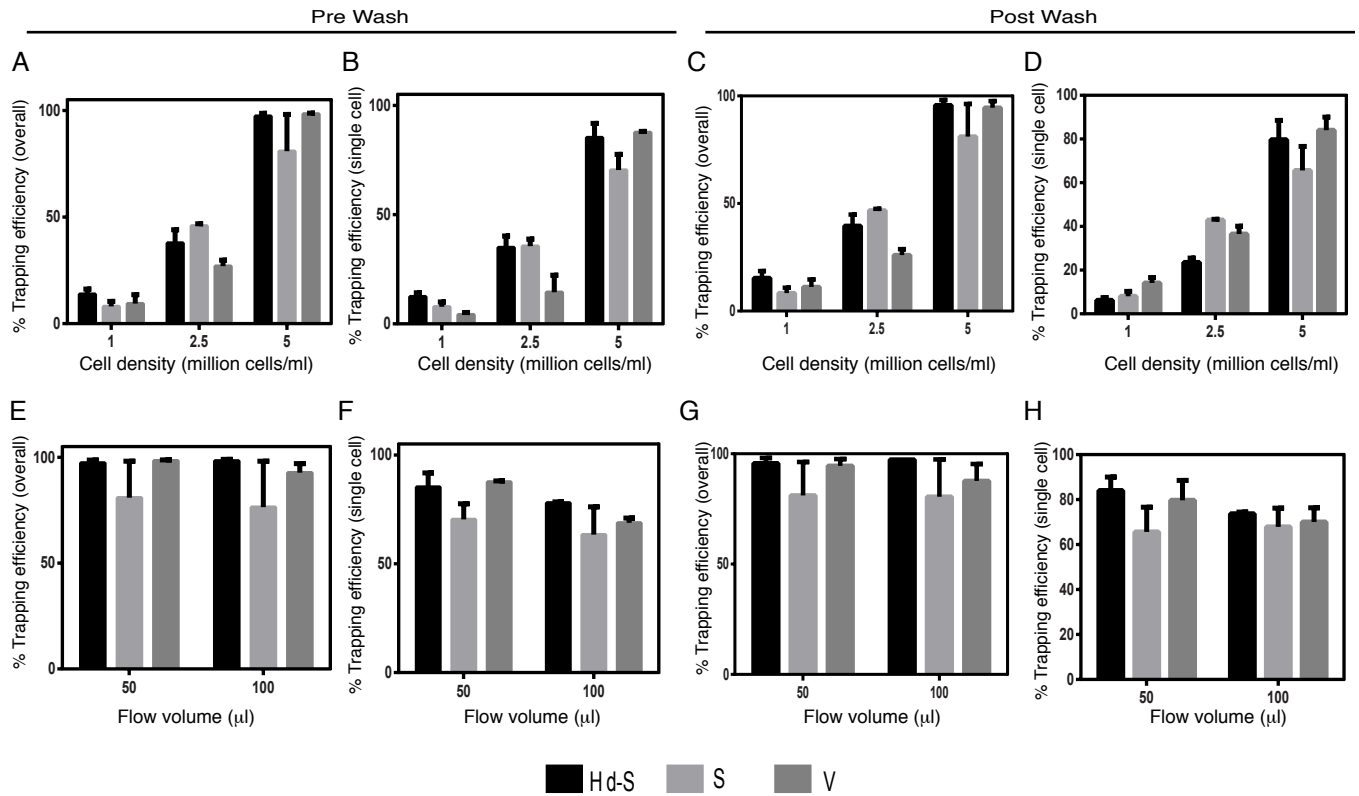


**Fig. S2.** Effect of cell loading density and volume on cell trapping efficiency. (A-B) Effect of varying cell density on (A) overall and (B) single-cell trapping efficiency for Hd-S, S and V traps. (C-D) Final trapping efficiency after a wash step to remove undocked cells. (E-F) Effect of inlet cell flow volume on (E) overall and (F) single-cell trapping efficiency for Hd-S, S and V traps. (G-H) Final trapping efficiency after a wash step to remove undocked cells. Data are presented as the mean  $\pm$  standard deviation of independent experiments (SD;  $n=2$ ).

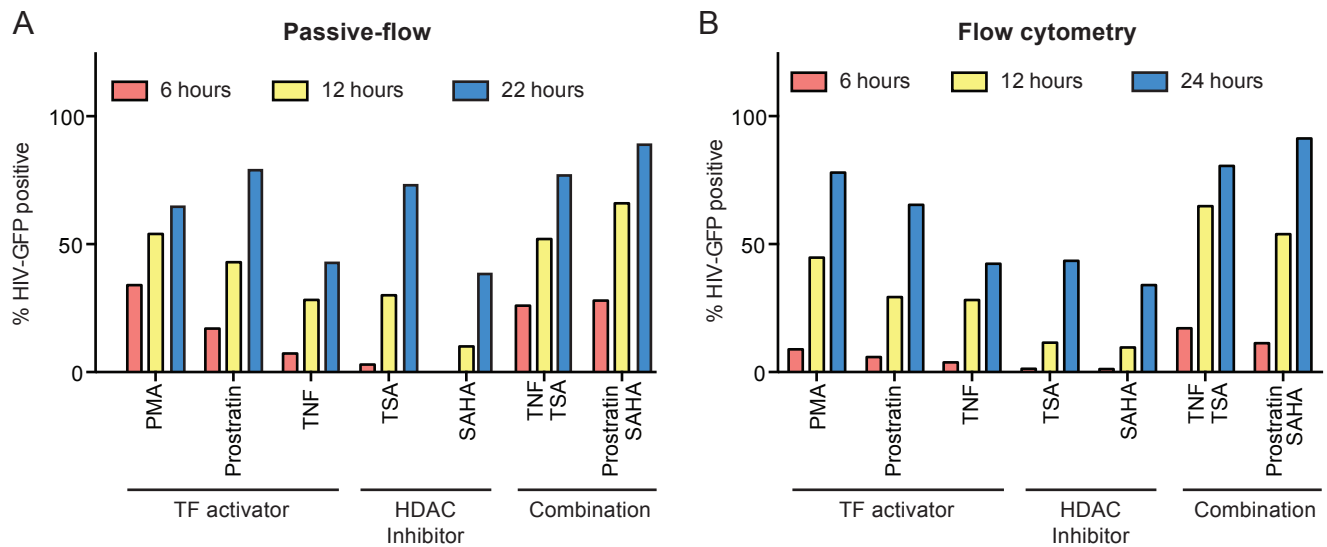


**Fig. S3.** Drug-stimulated latent HIV activation in the passive-flow device is similar to behavior observed in plate-based flow cytometry assays. (A) Bar graph of % HIV-GFP positive cells in response to indicated treatments in the passive-flow device. Fluorescence images for GFP were taken every 5 minutes after stimulation, and the number of GFP positive cells were counted at 6, 12 and 22 hours after stimulation. GFP positive cells calculated at 22 hours included cells that were locally displaced from the trap (up to 500  $\mu$ m) in order to record enough cells. (B) Bar graph of % HIV-GFP positive cells in response to indicated treatments in a cell-culture dish. Fluorescence was measured at 6, 12, and 24 hours after stimulation with flow cytometry. Data for 0 hours not shown because % HIV-GFP positive cells was less than 1% for both assays.

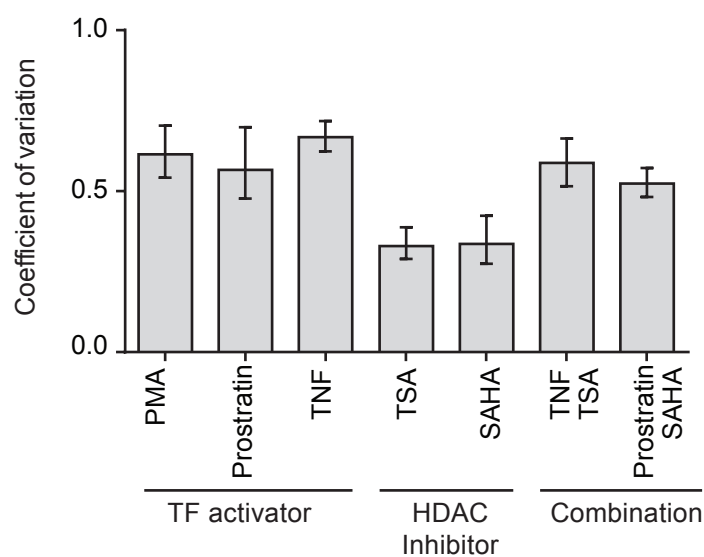


**Fig S4.** Trends in the CV for  $t_{on}$  are consistent at longer stimulation times. Jurkat cells were stimulated and observed for 22 hours in the passive-flow device. All cells that remained in the field of view for 22 hours were tracked, including cells that were locally displaced from the trap (up to 500  $\mu\text{m}$ ).

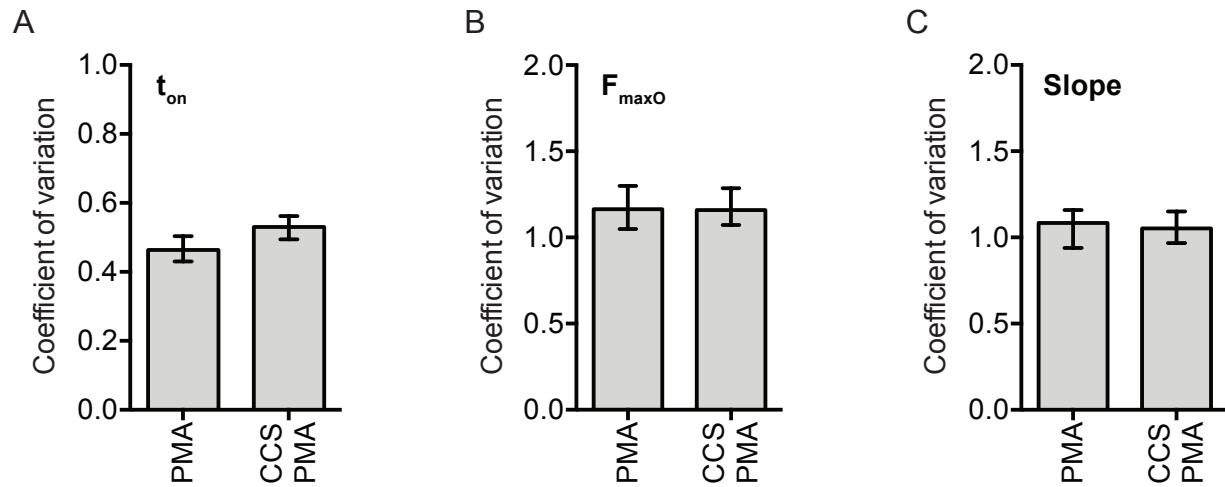


**Fig. S5.** CVs for  $t_{on}$ ,  $F_{maxO}$ , and slope are consistent between cell cycle synchronized and unsynchronized cells after 12 hours of PMA treatment. (A) Bar graph of coefficient of variation (CV) for onset of activation time ( $t_{on}$ ) for cell cycle synchronized cells versus unsynchronized cells after PMA treatment. (B) CVs for observed maximum expression ( $F_{maxO}$ ). (C) CVs for slope. Cells were synchronized for 24 hours via serum starvation prior to treatment with PMA. Error bars represent 95% confidence interval obtained by bootstrapping.

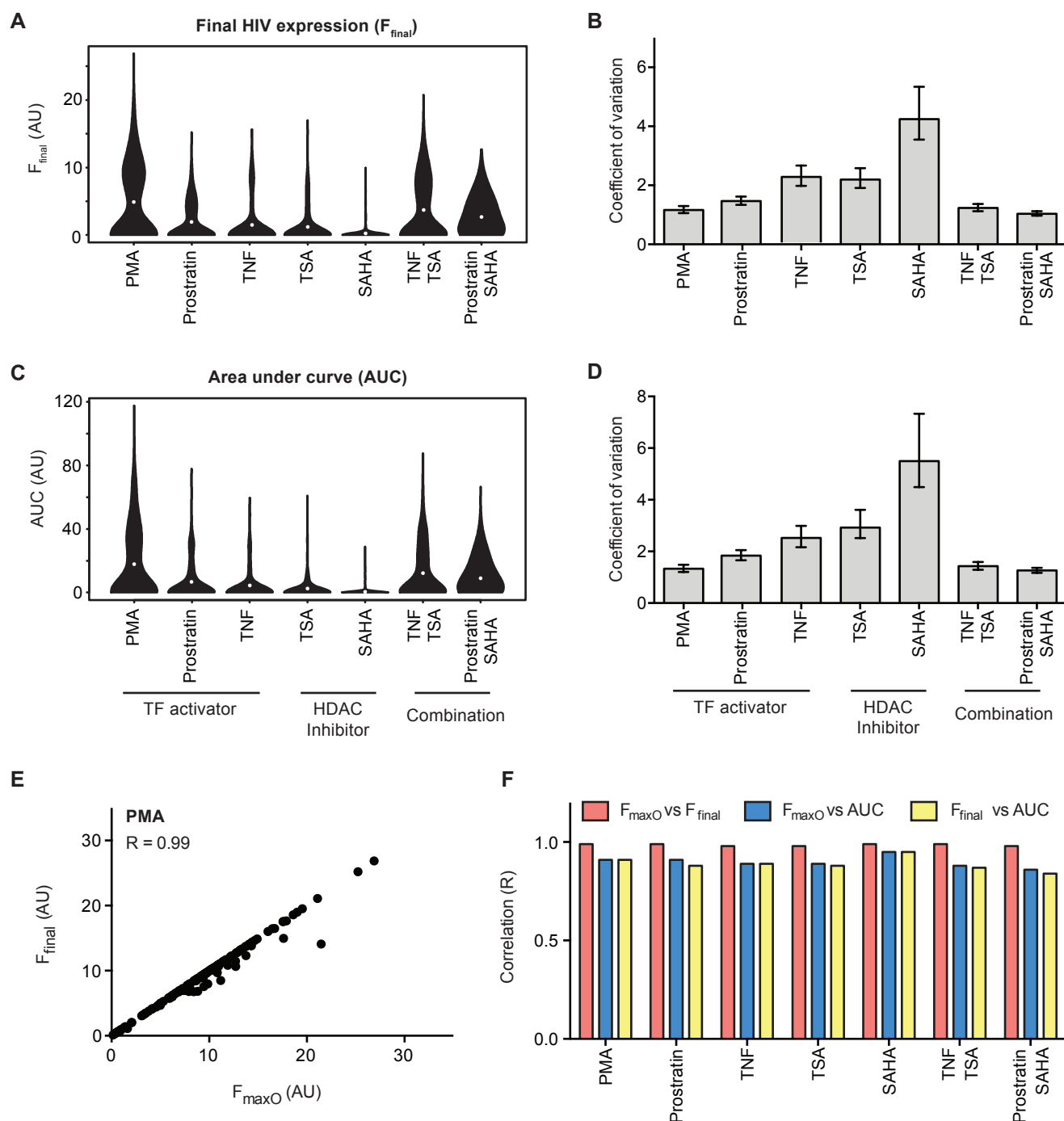


**Fig. S6.** Three metrics that describe HIV expression are strongly correlated. (A) Distributions of HIV expression at 12 hours of treatment ( $F_{final}$ ) for all cells ( $n \geq 230$ ). White dot indicates mean of distribution. (B) CV of final HIV expression. Error bars represent 95% confidence interval obtained by bootstrapping. (C) Distributions for AUC for HIV expression over time for all cells. (D) CV for AUC. (E) Example of scatterplot for correlation between  $F_{maxO}$  and  $F_{final}$  in cells activated by PMA treatment.  $R$  indicates Pearson correlation coefficient. (F) Bar graph for correlation between indicated metrics for each treatment.

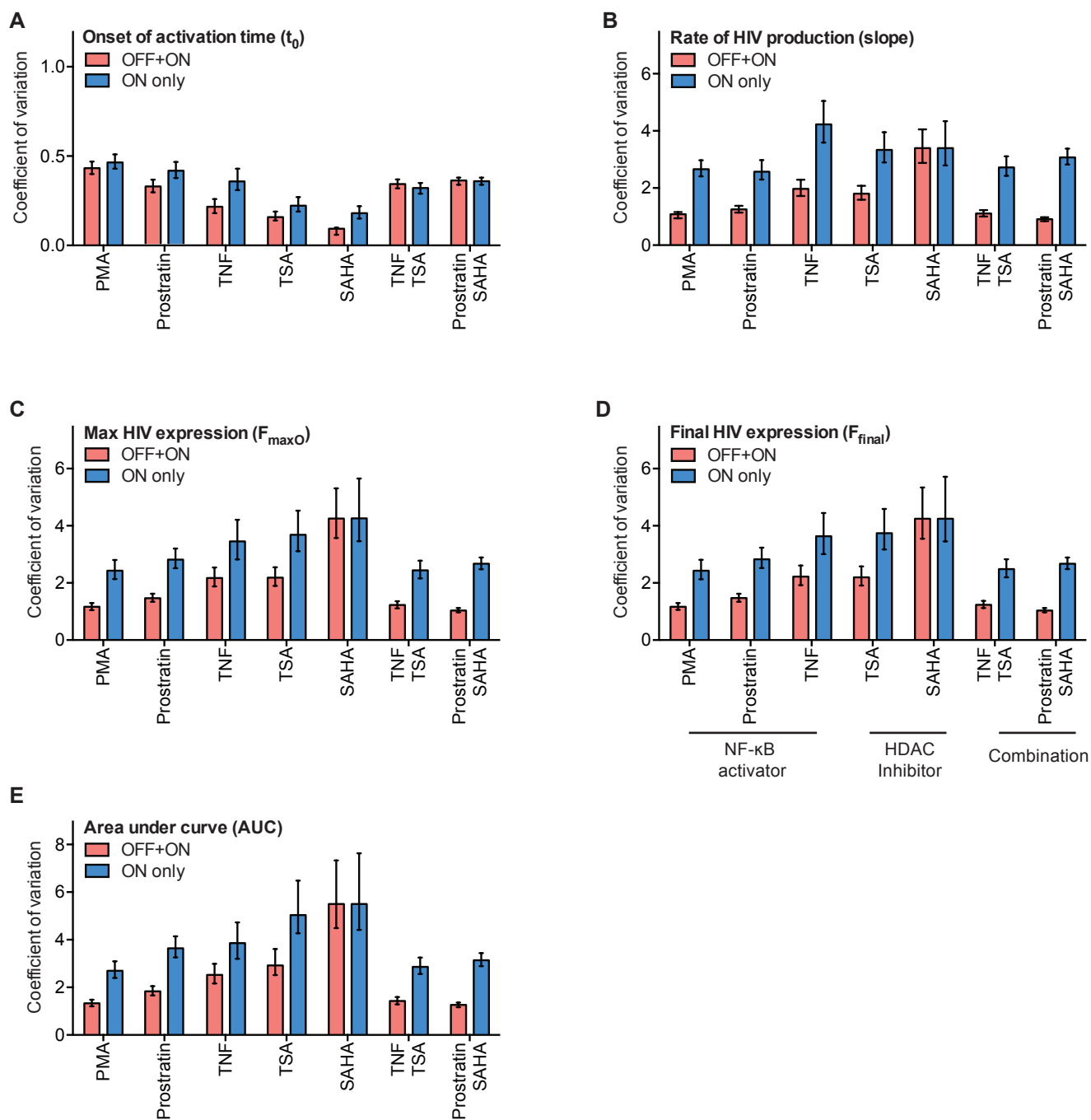


**Fig. S7.** Trends between different treatments are similar with and without the quantification of non-activators. (A) Bar graph for coefficient of variation (CV) for onset time for each treatment without (blue) and with (red) non-activators. (B-E) Bar graphs for CVs for (B)  $F_{\max O}$ , (C)  $F_{\text{final}}$ , (D) AUC, and (E) slope. For each metric, CVs for each perturbation were normalized by setting SAHA OFF+ON as the greatest CV, scaling SAHA ON to the same value, and applying the same scaling constant to the ON CV for each perturbation. CVs were normalized to demonstrate similarity in trends. Error bars represent 95% confidence interval obtained by bootstrapping.



**A**

Onset Time ( $t_{on}$ )	PMA	TNF	TSA	TNF+TSA	Pro	SAHA	Pro+SAHA
PMA		0.0001	0.0001	0.0001	0.0001	0.0001	0.0001
TNF			0.0546	0.0001	0.0224	0.0074	0.0038
TSA				0.0001	0.0001	0.15	0.0001
TNF+TSA					0.1	0.0001	0.0482
Prostratin						0.0001	0.93
SAHA							0.0001
Pro+SAHA							

**B**

Max ( $F_{maxO}$ )	PMA	TNF	TSA	TNF+TSA	Pro	SAHA	Pro+SAHA
PMA		0.0001	0.0001	0.0269	0.0001	0.0001	0.0034
TNF			0.95	0.0001	0.0004	0.0001	0.0001
TSA				0.0001	0.0001	0.0001	0.0001
TNF+TSA					0.0001	0.0001	0.5
Prostratin						0.0001	0.0001
SAHA							0.0001
Pro+SAHA							

**C**

Slope (S)	PMA	TNF	TSA	TNF+TSA	Pro	SAHA	Pro+SAHA
PMA		0.0001	0.0001	0.22	0.0001	0.0001	0.0071
TNF			0.77	0.0001	0.0016	0.0001	0.0001
TSA				0.0001	0.0001	0.0001	0.0001
TNF+TSA					0.0001	0.0001	0.1269
Prostratin						0.0001	0.0001
SAHA							0.0001
Pro+SAHA							

$\alpha = 0.0023$

**Table S1.** Analysis of distributions for (A) onset of activation time ( $t_{on}$ ), (B) maximum HIV expression ( $F_{maxO}$ ), and (C) rate of HIV production (slope) demonstrates that LRAs activate latent HIV with significantly different dynamics. Pairwise comparisons evaluated by Wilcoxon-Mann-Whitney test with Bonferroni correction.